Fermi National Accelerator Laboratory

FERMILAB-Pub-79/20-EXP
7340.319

(Submitted to Phys. Rev. Lett.)

MEASUREMENT OF NUCLEON STRUCTURE FUNCTION IN MUON SCATTERING AT HIGH q^2

R. C. Ball, D. Bauer, C. Chang, K. W. Chen
S. Hansen, J. Kiley, I. Kostoulas, A. Kotlewski,
L. Litt, P. F. Schewe
Michigan State University, East Lansing, Michigan 48824

and

A. Van Ginneken
Fermi National Accelerator Laboratory, Batavia, Illinois 60510

February 1979

MEASUREMENT OF NUCLEON STRUCTURE FUNCTION IN MUON SCATTERING AT HIGH q^2

R. C. Ball, D. Bauer, C. Chang[†], K. W. Chen
S. Hansen[††], J. Kiley, I. Kostoulas[††], A. Kotlewski*,
L. Litt*, P. F. Schewe**
Michigan State University
East Lansing, Michigan 48824

and

A. Van Ginneken
Fermi National Accelerator Laboratory
Batavia, Illinois 60510

ABSTRACT

The nucleon structure function, F_2, has been measured up to $q^2 = 120$ $(GeV/c)^2$ and for $40 < W^2 < 300$ GeV^2. The data exhibit a significant pattern of scaling violation. Compared to lower energy data, F_2 shows an observable increase of $\sim 15\%$ at high q^2 for $x < 0.4$. The pattern of the rise appears consistent with a threshold in the variable W.

Previous experiments[1-3] on deep inelastic muon and electron scattering have established significant deviations from Bjorken scaling[4] up to $q^2 = 50$ $(GeV/c)^2$. The nucleon structure function, $F_2(x,q^2)$, can no longer be expressed as a function of a single scaling variable, say x ($\equiv q^2/2M\nu$, where q^2 is the square of the four momentum transfer of the scattered muon, M the nucleon mass and $\nu \equiv E_0 - E'$, the difference in energy of incident and scattered μ). Theoretical interpretations[5] of non-scaling behavior include field-theoretic arguments, composite constituents of the nucleon, gauge theory of strong interactions with color degree of freedom (QCD), and new hadronic degrees of freedom in deep inelastic processes.

The present experiment, carried out at Fermilab, increases significantly the statistical certainty and the kinematical range over which deep inelastic muon scattering ($\mu N \rightarrow \mu X$) has thus far been explored. For 2×10^{10} incident muons with an energy of 270 GeV (μ^+ and μ^-), 10^6 deep inelastic events above $q^2 = 5$ $(GeV/c)^2$ are recorded. Results from a large fraction of the μ^+ exposure are reported. The target consisted of a 7.4 m long (4,260 g/cm^2) iron-scintillator calorimeter which also measured the final state hadron energy. Following the target was a 745 g/cm^2 thick steel hadron shield and a spectrometer[6] consisting of eight toroidal magnets (4,973 g/cm^2 thick and about 90 cm in radius). Both the hadron shield and spectrometer were interleaved with wire spark chambers. In addition, three vertical and horizontal trigger banks of scintillation counters were positioned within the spectrometer. Three scintillation counters (15.9 cm radius) centered on the beam axis formed a veto which eliminated events with a penetrating particle at a small angle. Proportional chambers and beam halo veto (scintillation) counters defined the incident muon.

The momentum of the scattered muon is determined from its trajectory through the magnetic spectrometer. Track finding efficiencies vary from 80% at low q^2 to

90% at high q^2 ($\geq$ 50 GeV$^2/c^2$). The resolution of the spectrometer was about 9%, with its central value calibrated to about 0.7%. The scattering angle is known to 0.4 mrad. The energy of the incident muon is determined to within 0.75%. The apparatus acceptance was relatively large (> 50%) for events having a scattered muon energy E' > 50 GeV and an angle 20 < θ < 80 mrad. Fig. 1 shows curves of equal apparatus acceptance in the q^2 - ν plane. Also shown are lines of constant W^2 ($\equiv 2M\nu - q^2 + M^2$), the square of the center-of-mass energy of the virtual photon-nucleon system.

The values of the structure function, F_2 per nucleon, were obtained from comparing the data to Monte Carlo predictions based on fits[7] of lower energy data in F_2^{ep} and F_2^{eD} and, with nearly the same result, using a QCD parametrization[8]. The calculation included effects of real incident beam distributions, Fermi motion of the nucleons in the iron nucleus, radiative corrections and wide-angle bremsstrahlung in simulating deep inelastic scattering. Incident and scattered muons are traced through the apparatus undergoing simulated magnetic deflection, multiple Colulomb scattering, μ - e scattering, bremsstrahlung and collision losses. Further analysis treats data and Monte Carlo events identically. The data presented below show only statistical errors and do not include relative systematic and normalization uncertainties estimated to be less than 10%.

Fig. 2 shows $F_2(\bar{x}_i,q^2)$ versus q^2 for successive x regions, where $\bar{x}_i$ is the weighted average of x for the i^{th} data point. Also shown are QCD predictions[8] both for $F_2(\bar{x}_i,q^2)$ (the solid curve Λ = 0.5) and for $F_2(\tilde{x},q^2)$ (the dash dotted curve, Λ = 0.5, dashed curve, Λ = 0.4) where $\tilde{x}$ is the weighted average value for the entire x region. For lower x regions (< 0.4), the data show a consistent pattern of near agreement with QCD at low q^2 and a tendency to rise above QCD at higher q^2. In Fig. 3 (a-h), the ratio R [$\equiv F_2(\bar{x}_i,q^2)/F_2(\bar{x}_i,q^2)_{QCD}$] is plotted versus ln q^2 for successive x cuts. The values of R for SLAC-MIT data,[3] calculated

in a similar manner, are also shown. The ratio of the QCD prediction for $\Lambda = 0.4$ GeV/c to that for $\Lambda = 0.5$ GeV/c is shown as a dashed line. In Fig. 3 (c-f) where the data disagree with the QCD prediction, the difference due to this change of Λ is not significant. This behavior of F_2 versus q^2 at a fixed x is statistically consistent with that expected from a threshold behavior in the variable W^2.

In Fig. 4, R is plotted against W^2 for all q^2 and x. Beyond $W^2 = (80 \pm 10)$ GeV^2, $R(W^2)$ is consistent with a rise of 12-15% above the lower W^2 data. Table I shows sample tests of a possible W^2-threshold behavior. The data are fit by a) a straight line, b) two separate straight lines on either side of $W^2 = 80$, and c) two separate constants. Both b) and c) are favored over a). A QCD prediction[8] is also tested.

This observed behavior of F_2 in q^2 or W^2 cannot be accounted for by known systematic effects which include uncertainties in measurement of E_0, E' and θ, variation in σ_S/σ_T[9] or in the application of radiative corrections and corrections for wide-angle bremsstrahlung and Fermi motion. The apparatus acceptance is a smooth function in W^2 and cannot accommodate a point-to-point rapid variation of F_2 in the range $65 < W^2 < 95$ GeV^2. Although $F_2(x,q^2)$ can conceivably be more closely fitted by readjustments of q_c^2, Λ, quark or gluon distributions in QCD, the observed q^2 or W^2 variation is not easily accommodated without major new assumptions since $F_2(q^2)|_x$ should be monotonic in q^2 or W^2, in contrast to the observed trend in this experiment.[10]

We acknowledge the staff of Fermilab for their support. We thank K. Thorne and M. Ghods for their help in data reduction. One of us (K.H.C.) would like to thank E. Lehman for useful discussions. This research was supported in part by the National Science Foundation under Grant No. 60950 and by the Department of Energy under Contract No. E(11-1)-1764.

†Present Address: Nat. Central Univ., Chung-Li, Taiwan, Repub. of China.

††Present Address: FNAL, Batavia, Illinois 60510.

*Present Address: Univ. of Miami School of Medicine, Biscayne Annex, Miami, FL 33152.

**Present Address: Brookhaven Nat. Lab., Upton, NY 11973.

1. C. Chang et al., Phys. Rev. Lett. 35, 901 (1975).

2. H. L. Anderson et al., Phys. Rev. Lett. 38, 1450 (1976); ibid. Phys. Rev. Lett. 41, 615 (1978).

3. E. M. Riordan et al., SLAC Report No. SLAC-PUB-1634, 1975 (unpublished).

4. J. D. Bjorken, Phys. Rev. 179, 1547 (1969).

5. e.g. H. Cheng and T. T. Wu, Phys. Rev. Lett. 22, 1409, (1969); K. Matsumoto, Progress Theor. Phys. 47, 1975 (1972); M. S. Chanowitz and S. D. Drell, Phys. Rev. Lett. 30, 1975 (1973); H. D. Politzer, Physics Reports 14c (1974) and references therein; M. Y. Han Y. Nambu, Phys. Rev. 139, B1006 (1965); J. C. Pati and A. Salam, Phys. Rev. Lett. 36, 11 (1976).

6. K. W. Chen, in Proceedings of the 1977 International Symposium on Lepton and Photon Interactions at High Energies, edited by F. Gutbrod (DESY, Hamburg, Germany) p. 467.

7. S. Stein et al., Phys. Rev. D12, 1884 (1975).

8. A. Buras and B. G. F. Gaemers, Nuclear Phys. B132 (1978); and private communication. The parton distributions for the proton with a scale parameter $\Lambda = 0.5$ GeV/c at $q_0^2 = 2$ (GeV/c)^2 are $xS = (1-x)^8$, $xG = 2.41\ (1-x)^5$, $xC = 0$, $xu_v = \frac{3}{B(0.7,3.6)} x^{0.7}(1-x)^{2.6}$ and $xd_v = \frac{1}{B(.85,4.35)} x^{0.85}(1-x)^{3.35}$. For the neutron, u_v and d_v distributions are interchanged. $\Lambda = 0.5$ GeV/c is preferred by recent fits to lepton scattering data.

9. F_2 is extracted assuming $R\ (\equiv \sigma_S/\sigma_T) = 0.25$. By assuming $R = 0.44$, the variation of the cross section is less than 2% for the range of the data presented here.

10. In QCD, the moment integrals $M_n(q^2) = \int_0^1 dx\, x^n[F_2(x,q^2)]$ vary as $\frac{a_n}{(\ln \frac{q^2}{\Lambda^2})^{b_n}}$, where a_n, b_n and Λ are constants. For a fixed x, $\frac{\partial F_2(x,q^2)}{\partial \ln q^2}$ is constant. Thus $F_2(q^2)$ varies montonically in q^2.

TABLE I

Fits to $R = a(W^2) + b$

W^2 Region	a ($\times 10^4$)	b	χ^2/DOF
All W^2	2.64 ± 0.66	1.058 ± 0.011	96.3/27
$W^2 < 80$ [1]	-0.72 ± 9.52	1.030 ± 0.058	11.3/5
$W^2 > 80$	-2.11 ± 0.91	1.159 ± 0.017	25.8/20
All W^2	0 [2]	1.097 ± 0.005	112.4/28
$W^2 < 80$ [1]	0 [2]	1.025 ± 0.010	11.3/6
$W^2 > 80$	0 [2]	1.121 ± 0.006	31.2/21
All W^2	0 [2]	1.00 [3]	485.4/29

1) The choice of $W^2 = 80$ GeV^2 is dictated by the best possible fit. χ^2/DOF improves further when resolution effects are included.

2) The slope is set to zero, i.e. R = constant.

3) Ratio of measured F_2 to QCD prediction of Ref. 8.

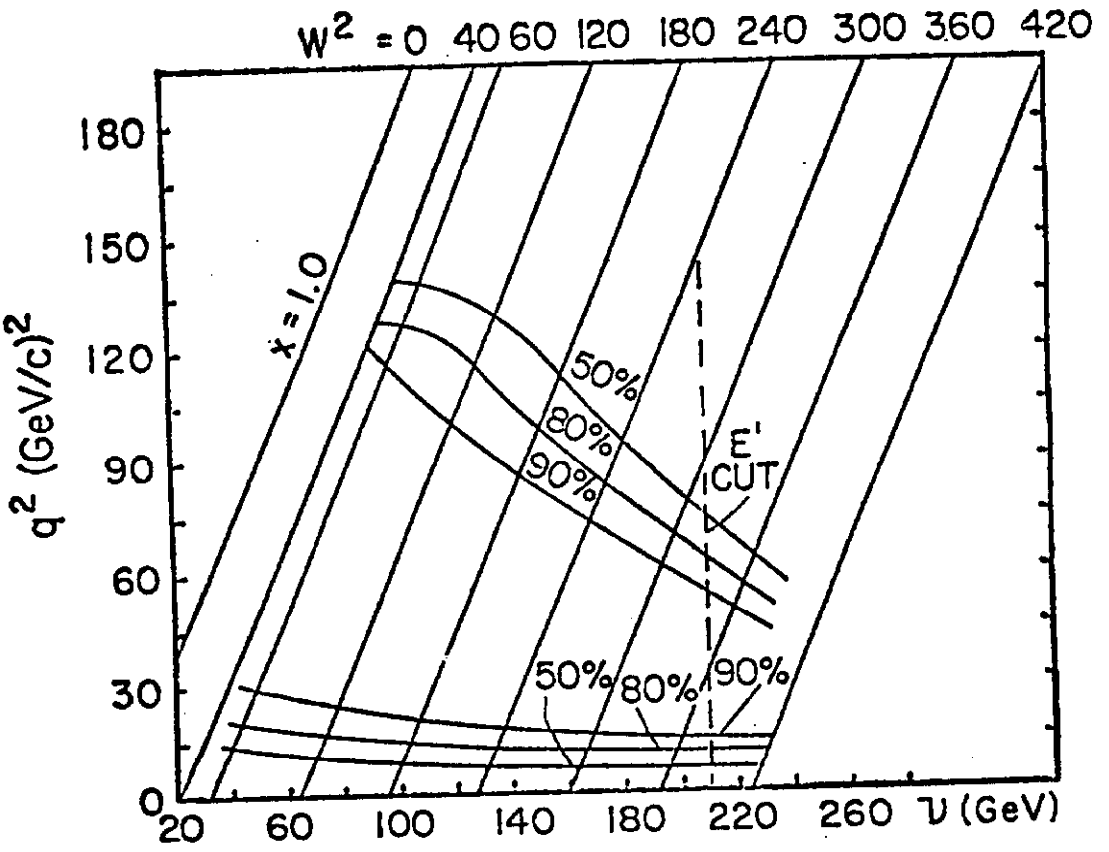

Fig. 1. Contour plot of apparatus acceptance as a function of q^2 and ν. Also shown are lines of constant W^2.

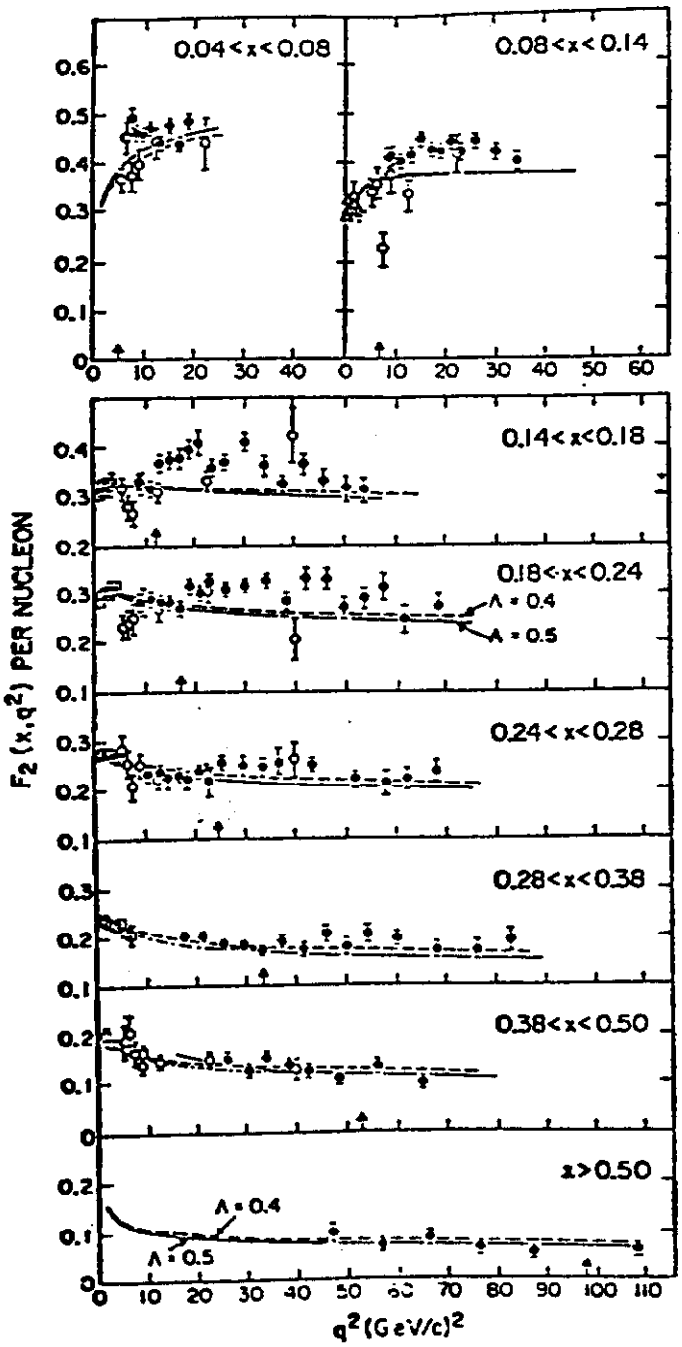

Fig. 2. Nucleon structure function F_2 versus q^2 for eight bands of x. Shown also are $F_2^{eD}/2$ (open square) of Ref. 3, and $F_2^{\mu p}$ of Ref. 2 (open circle) corrected for n - p differences. The solid, dashed, and dash-dotted lines are QCD predictions as explained in the text. The value $W^2 = 80$ GeV^2 is indicated by arrows. Errors are statistical.

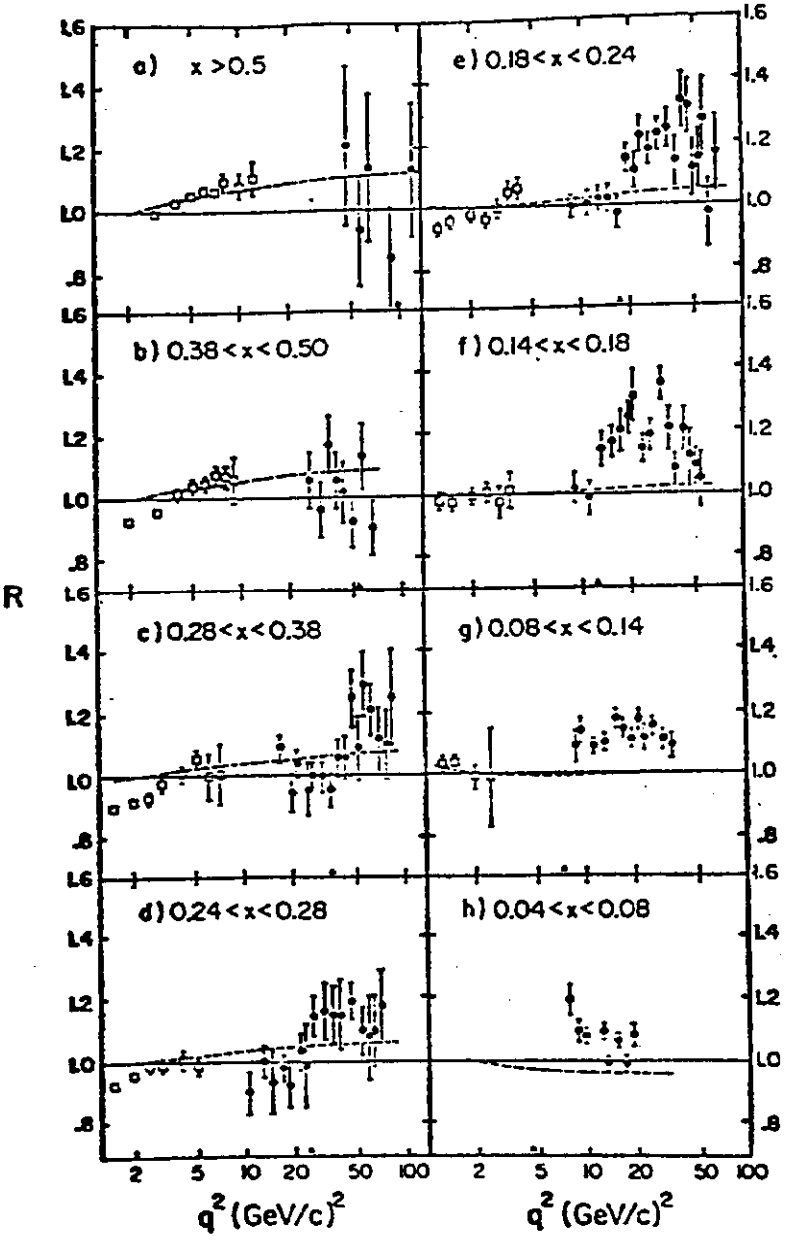

Fig. 3. Ratio of observed to calculated (QCD) structure function (Λ = 0.5 GeV) versus q^2 for eight bands of x. The value W^2 = 80 GeV^2 is indicated by arrows. The dashed line is the ratio of the QCD prediction for F_{2}^{eD} Λ = 0.4 to that for Λ = 0.5 GeV/c. Open squares show ratio for

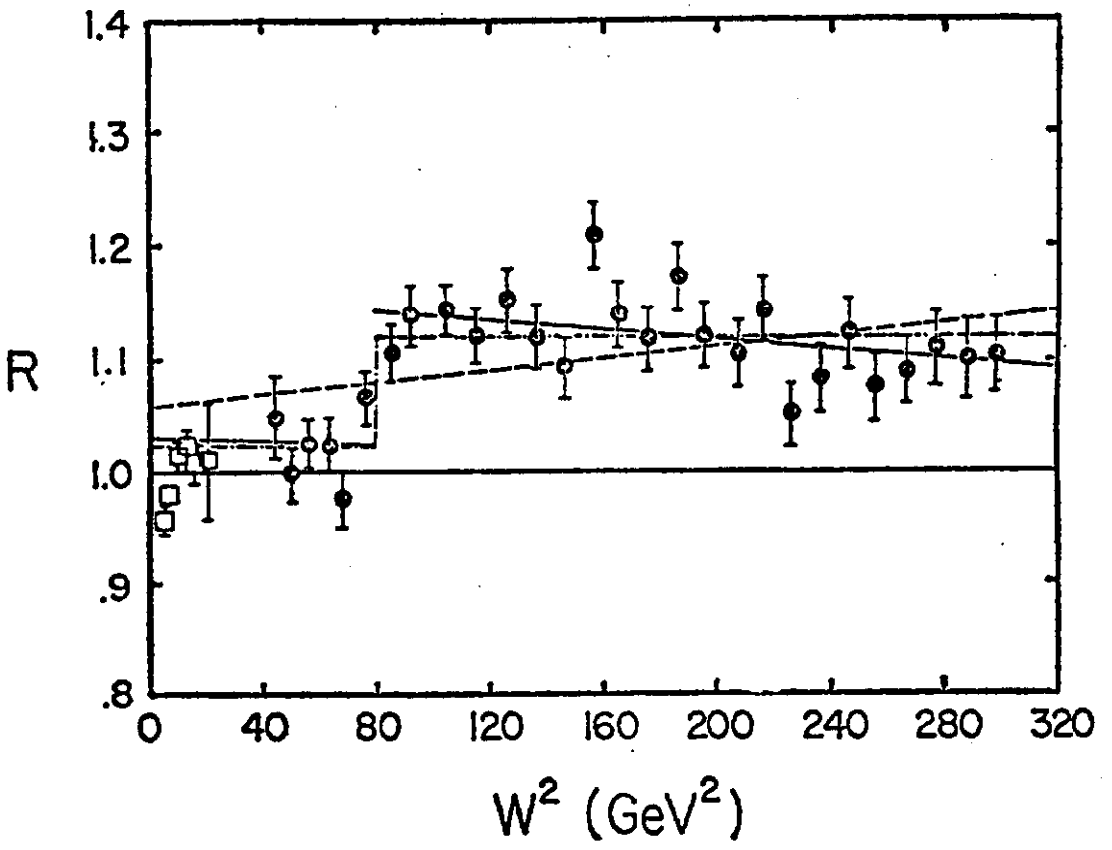

Fig. 4. R, ratio of observed to calculated (QCD) structure function, versus W^2, for all q^2 and x. Shown are fits to a) $R = a(W^2) + b$ (dashed line) b) separate lines for the range $80 < W^2$ and $W^2 < 80$ GeV^2 (solid lines) and c) two separate constants (dash-dotted line). $F_2^{eD}/2$ data [$q^2 > 2.0$ (GeV/c)^2] (Ref. 3) are shown (open square) but not fitted.